Research Article | Vol. 11, No. 11 / 1 Nov 2021 / Optical Materials Express 3801
Optical Materials EXPRESS

Electro-optical properties of doped polymers with high transparency in the visible wavelength range

CLAUS VILLRINGER,[1,2,*] PATRICK STEGLICH,[1,3] SILVIO PULWER,[1] SIGURD SCHRADER,[1] AND JAN LAUFER[2]

[1]Technische Hochschule Wildau, Hochschulring 1, 15745 Wildau, Germany
[2]Institut für Physik, Martin-Luther-Universität Halle-Wittenberg, von-Danckelmann-Platz 3, 06120 Halle (Saale), Germany
[3]IHP - Leibniz-Institut für innovative Mikroelektronik, Im Technologiepark 25, 15236 Frankfurt (Oder), Germany
[*]villringer@th-wildau.de

Abstract: The electro-optical (EO) properties of poly(methyl methacrylate) and the photopolymer poly(vinyl cinnamate) doped with varying concentrations of the EO chromophore 2-Methyl-4-nitroaniline were measured. The EO polymers were embedded in Fabry-Pérot etalons for the simultaneous determination of the Pockels and Kerr coefficients from measurements of the fringe shift induced by an external electric field. It was found that the host polymer has a significant impact on the EO performance and that the undoped host polymers exhibit a significant Pockels effect. Moreover, the Kerr effect provides a substantial contribution of 27% to the total change of the refractive index at relatively high electric field strengths of $E = 91.2\,\mathrm{MV\,m^{-1}}$.

1. Introduction

The refractive index of electro-optic (EO) polymers can be changed by an external electric field due to a combination of the Pockels and Kerr effect. In guest-host systems, which consist of a matrix polymer and embedded EO chromophores, the Pockels effect relies on a preferential spatial orientation of the electrically polarizable EO chromophore, which is typically induced by poling the EO polymer material at elevated temperatures while an external field is applied. The properties of EO chromophores, which are composed of electron donor and acceptor groups interacting through a π-electron conjugation bridge, are an important factor in the design of EO polymers. To maximise the Pockels effect, polymers with a high glass transition temperature and EO chromophores of comparatively large molecular size are advantageous as they provide optimal orientational stability [1] which has been achieved not only in guest-host systems but also in materials where the EO chromophores are covalently bound to the host polymer [2]. Orientational stability can also be improved by thermal [3] or photochemical [4] crosslinking of the host polymer during the poling process.

EO polymers have been explored for applications in the telecommunications sector [5–7] where their fast temporal response, low optical losses, high EO activity, stability and ease of processing has been exploited for example in the development of spatial light modulators (SLM) [8]. As a result, most of the recent research activity has been focussed on the development of EO polymers for the near infrared wavelength range [9–12]. While there are comparatively few reports on EO polymers for the visible range, future applications of such materials may lie in tuneable optical filters and in the optical detection of ultrasound, for example in the form of tuneable Fabry-Pérot (FP) sensors for biomedical photoacoustic (PA) imaging studies [13–16]. For such applications, new EO polymers are required that are highly transparent in the visible wavelength region. Conventional near-infrared EO chromophores are not suitable despite their typically high

#435953 https://doi.org/10.1364/OME.435953
Journal © 2021 Received 4 Jul 2021; revised 19 Aug 2021; accepted 24 Aug 2021; published 20 Oct 2021

Optical Materials EXPRESS

EO activity [3], as they result in strong optical absorption in the visible range. While a range of EO chromophores for the visible wavelength region have been reported [1,17–20], they tend to show weaker EO effects which is primarily due to the smaller size of the π-electron conjugated system [17].

In this study, EO polymers were developed and the linear and nonlinear optical properties of poled and unpoled guest-host systems were measured as a function of chromophore concentration. Furthermore, the influence of the host polymer on the EO activity was investigated. To measure the Pockels and Kerr effect, the polymers were used as spacer material in FP etalons formed by two distributed Bragg reflectors (DBR). Since the DBR thickness reduces the effective field strength inside the polymer, the number of DBR layers between the electrodes and the EO polymer was varied.

2. Theoretical model of EO polymers in an FP etalon

The refractive index of EO polymers can be actively controlled using an external electric field. Taking into account the linear and quadratic EO effect, the refractive index change perpendicular to the electric field strength E can be expressed as

$$\Delta n_{\mathrm{EO}} = -\frac{1}{2} n_{\mathrm{EO}}^3 r_{13} E - \frac{1}{2} n_{\mathrm{EO}}^3 R_{13} E^2, \tag{1}$$

where r_{13} is the Pockels coefficient, R_{13} is the Kerr coefficient and n_{EO} is the unperturbed refractive index of the EO polymer [21]. In general, EO activity in polymers requires the presence of active dipolar molecules, which can be an inherent feature of some undoped matrix materials or be introduced by adding EO chromophores. In EO polymers with a molecular centrosymmetric orientation, the dipolar molecules are isotropically oriented. In this case, which may also apply to the undoped polymer matrix material, only the Kerr effect is observed and the change in refractive index is proportional to the square of the electric field strength as shown schematically in Fig. 1(a). By contrast, polymers in which the EO chromophores possess a preferential spatial orientation, which is also referred to as acentric molecular order [11], show both Pockels and Kerr effect as shown schematically in Fig. 1(b). This effect is also observed in some undoped host polymer materials due to the presence of permanent dipoles [22]. Here, the field-induced refractive index change is dominated by the linear Pockels effect. At low electric field strengths, the Kerr effect can therefore be neglected.

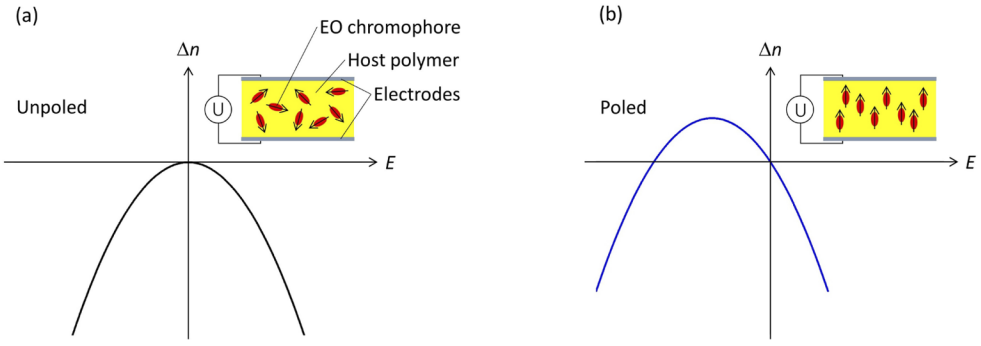

Fig. 1. Refractive index change as a function of the electric field strength E of an (a) unpoled EO polymer with isotropic molecular order and (b) poled EO polymer with acentric molecular order.

The acentric molecular order of the EO chromophores is usually induced using electric field poling, which involves heating the polymer above the glass transition temperature whilst

Optical Materials EXPRESS

applying an electric field to which the EO molecules align. The material is then cooled to room temperature while the electric field is maintained. As a result, the field-induced orientation of the EO chomophores is preserved. If a smaller electric field than the poling field is then applied to the poled polymer, the refractive index changes approximately linearly with E. By contrast, for field strengths that are comparable to that of the poling field, linear and nonlinear changes due to the Pockels and Kerr effect are observed as shown in Fig. 1(b).

To measure small electrically induced changes in refractive index, which are typically in the range of $\Delta n_{\mathrm{EO}} \approx 10^{-4}$, FP etalons provide a sensitive detection method as the small refractive index changes result in a large shift in the resonance wavelength. In this study, FP etalons which consisted of two dielectric mirrors and an EO polymer spacer were fabricated. The electric field was generated by a voltage U applied to two electrodes placed on either side of the FP etalon. The electric field strength in the EO polymer film is given by

$$E = \mu \frac{U}{d_{\mathrm{EO}}}, \tag{2}$$

where d_{EO} is the layer thickness of the EO polymer film. Provided the electrodes are located outside the resonator and dielectric materials are used to fabricate the mirrors, the electric field strength in the EO polymer spacer is reduced by the effective voltage ratio μ, due to the voltage drop across the mirrors. μ is obtained using

$$\mu = \frac{U_{\mathrm{eff}}}{U} = \frac{d_{\mathrm{EO}}/\sqrt{\varepsilon_{\mathrm{r,EO}}}}{d_{\mathrm{EO}}/\sqrt{\varepsilon_{\mathrm{r,EO}}} + \sum_{i=1}^{N_{\mathrm{L}}} d_{\mathrm{L}}/\sqrt{\varepsilon_{\mathrm{r,L}}} + \sum_{i=1}^{N_{\mathrm{H}}} d_{\mathrm{H}}/\sqrt{\varepsilon_{\mathrm{r,H}}}}, \tag{3}$$

where U_{eff} is the effective voltage applied to the EO polymer, $\varepsilon_{\mathrm{r,EO}}$ is its relative dielectric constant and $\varepsilon_{\mathrm{r,L}}$, $\varepsilon_{\mathrm{r,H}}$, d_{L}, d_{H}, N_{L}, N_{H} are the relative dielectric constants, layer thicknesses and number of layers of the dielectric materials with low and high refractive index [23]. If the spacer thickness is significantly larger than the interrogation wavelength λ, the thickness of the EO polymer film can be approximated using

$$d_{\mathrm{EO}} = \frac{\lambda^2/\Delta\lambda_{\mathrm{FSR}} - \lambda}{2n_{\mathrm{EO}}}, \tag{4}$$

where $\Delta\lambda_{\mathrm{FSR}}$ is the free spectral range at normal incidence. The dispersion of the refractive index of the EO polymer and the spectral phase dispersion are neglected.

Small changes in the optical thickness of the spacer cause a shift in the centre wavelength of the interferometer resonance which can be calculated using

$$\Delta\lambda = \frac{(2d_{\mathrm{EO}} - \frac{\lambda}{\pi}\frac{\partial\Phi}{\partial n_{\mathrm{EO}}})\Delta n_{\mathrm{EO}} + 2n_{\mathrm{EO}}\Delta d_{\mathrm{EO}}}{\frac{2n_{\mathrm{EO}}d_{\mathrm{EO}}}{\lambda} + \frac{\lambda}{\pi}\frac{\partial\Phi}{\partial\lambda}}, \tag{5}$$

where $\partial\Phi/\partial n_{\mathrm{EO}}$ and $\partial\Phi/\partial\lambda$ are the phase dispersions with respect to the refractive index of the EO polymer and interrogation wavelength [23], respectively, and can be calculated using the matrix method [24]. Δn_{EO} is the change in the refractive index caused by EO effects and Δd_{EO} the change in the physical thickness due to electro-mechanical effects.

The shift in the resonant wavelength $\Delta\lambda(U)$ was measured as a function of the voltage U. A second order polynomial regression model given by

$$\Delta\lambda(U) = C_1 U + C_2 U^2 \tag{6}$$

was fitted to the measured data by varying C_1 and C_2. The Pockels coefficient r_{13} and the Kerr coefficient R_{13} were calculated from the fitted values of C_1 and C_2 by combining Equations (1, 2,

Optical Materials EXPRESS

5, 6) to yield

$$r_{13} = -\frac{2C_1 d_{\mathrm{EO}}}{n_{\mathrm{EO}}^3 \mu A} \tag{7}$$

and

$$R_{13} = -\frac{2C_2 d_{\mathrm{EO}}^2}{n_{\mathrm{EO}}^3 \mu^2 A}, \tag{8}$$

with

$$A = \frac{2d_{\mathrm{EO}} - \frac{\lambda}{\pi}\frac{\partial \Phi}{\partial n_{\mathrm{EO}}}}{\frac{2n_{\mathrm{EO}} d_{\mathrm{EO}}}{\lambda} + \frac{\lambda}{\pi}\frac{\partial \Phi}{\partial \lambda}}. \tag{9}$$

The electro-mechanical effects are neglected in this model, as they cannot be separated from the EO effects using the measurement method presented in this paper.

3. Methods

The linear optical properties of EO polymers were measured using spectroscopic ellipsometry. The polymers were embedded in FP etalons to measure the electrically induced fringe shift from which the Pockels coefficient, the Kerr coefficient and the refractive index change were determined. Measurements were made in poled and unpoled EO polymers. The influence of the EO chromophore concentration, the host polymer and the dielectric layers between the electrodes and the EO polymer were also investigated.

3.1. Sample preparation

Guest-host systems were used to form EO polymers. The host polymers consisted of either the photopolymer Poly(vinyl cinnamate) (PVCi) or poly(methyl methacrylate) (PMMA). PVCi was chosen as it offers the additional option of tuning the refractive index using photochemical crosslinking [25,26]. This process is irreversible but may allow the fabrication of FP etalons of high homogeneity of thickness, which is of interest in parallelised ultrasound detection schemes used in metrology and imaging applications [13–15]. The EO chromophore 2-Methyl-4-nitroaniline (MNA) was used due to its commercial availability and negligible absorption in the visible spectral range. PMMA (Sigma Aldrich) with a molecular weight of Mw = 996,000 and MNA (Tokyo Chemical Industry) were dissolved in 1.1.2.2-tetrachloethane (Sigma Aldrich). PVCi (Sigma Aldrich) and MNA were dissolved in N-Methyl-2-pyrrolidone (Sigma Aldrich). The polymer solutions were stirred for 24 h and filtered through a PVDF-membrane with 0.2 µm pore size (Carl Roth).

For the measurement of the linear optical properties, the polymer solutions were deposited on silicon substrates using spin coating to form layers with a thickness of approximately $d_{\mathrm{EO}} \approx 300$ nm. To remove the solvent, the samples were placed on a hot plate with a temperature of 50 °C for 30 min for prebake and in a vacuum oven at 70 °C for three days.

The nonlinear optical properties of the EO polymers were measured using a setup based on FP etalons, a schematic of which is shown in Fig. 2(a). The etalons were fabricated layer by layer to produce a structure consisting of EO polymer spacers with a thickness of about $d_{\mathrm{EO}} \approx 5$ µm placed between two DBR and two transparent indium tin oxide (ITO) electrodes. The DBR consist of alternating layers of silicon dioxide (SiO_2) and titanium dioxide (TiO_2). The ITO electrode is part of the mirror design and serves as first high-index layer. The thickness of the layers were $d_{\mathrm{ITO}} = 65.5$ nm, $d_{\mathrm{SiO_2}} = 92.0$ nm and $d_{\mathrm{TiO_2}} = 54.8$ nm, respectively, and were chosen to achieve high reflectivity at $\lambda = 538$ nm. DBRs with a total of either four or eight layers were deposited.

To investigate the dependence of the EO properties on chromophore concentration, PVCi was doped with MNA at concentrations ranging from 0 wt% to 15 wt%. FP etalons were prepared

Optical Materials EXPRESS

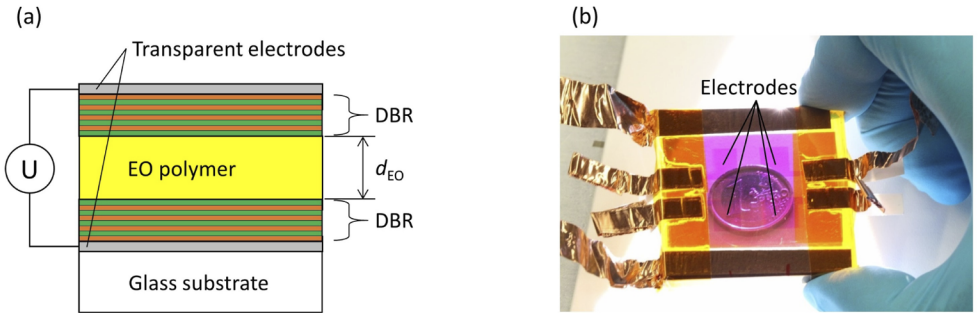

Fig. 2. (a) Schematic of the FP etalons which consisted of an EO polymer spacer, transparent ITO electrodes and DBRs. (b) Photograph of an FP etalon. The ITO electrodes were contacted using conductive copper adhesive tape. The upper ITO electrode was divided into four regions.

by depositing an ITO layer as a ground electrode and a DBR consisting of eight alternating SiO_2 and TiO_2 layers onto a Borofloat 33 glass substrate using reactive magnetron sputtering. The number of layers was chosen to obtain a reflectivity between $R = 0.96$ and $R = 0.98$ in the spectral range of 500 nm to 575 nm. The polymer solutions were spin coated onto the DBR at 1400 rpm and dried as described above to produce layers with a thickness of about 5 μm. The upper DBR and ITO layer were also deposited using magnetron sputtering. The upper ITO layer was divided into four separate electrodes each covering an area of approximately 8 mm x 8 mm to create multiple etalon samples. The ITO electrodes were contacted using conductive copper adhesive tape. Figure 2(b) shows a photograph of an FP etalon.

Contact poling was used to align the EO chromophores in the doped polymers to an external electric field. The FP etalons were placed on a hot plate and heated to the glass transition temperature of the polymers while an electrical voltage of −600 V was applied to the electrodes. Temperature and electrical voltage were maintained for 30 min after which the samples were allowed to cool to room temperature while the electric field was maintained.

To investigate the effect of the host polymer on the EO properties, pure PMMA and PMMA doped with 10 wt% of MNA were used as FP spacer materials. The sample preparation and the layer structure of the FP etalons are identical to those described above.

To study the influence of the voltage drop across the DBR and to verify the Equation (3), etalons were prepared with DBR of different reflectivities, i.e. a different number of dielectric layers between the electrodes and the EO polymer spacer. DBRs consisting of eight and four layers were deposited. Additional samples were prepared in which the DBR consisted of eight layers and where the ITO electrodes are directly in contact with the EO polymer spacer. PVCi doped with 10 wt% of MNA was used as spacer material.

3.2. Measurement and data analysis

The refractive index n and the extinction coefficient k were measured in EO polymer films on silicon substrates using spectroscopic ellipsometry (Sentech SE 850). The optical properties of the EO polymer were modelled using the Bruggemann effective medium approximation [27]. A Cauchy model [28] was employed to describe the transparent polymer matrix and the Tauc-Lorentz oscillator model [29] to describe the EO chromophore (MNA).

The experimental setup for measuring the nonlinear optical properties of the EO polymers within FP etalons is shown schematically in Fig. 3(a). A fiber-coupled LED (M530F2, Thorlabs) was connected to a 50:50 fiber optic coupler (TM200R5S1B, Thorlabs). An aspheric achromatic lens (49-658, Edmund Optics) was used to focus the light at normal incidence onto the sample.

Optical Materials EXPRESS

The reflected intensity was recorded using a spectrometer (HR4000, Ocean Optics). The interferometer transfer function (ITF), which describes the change in the reflected optical power as a function of wavelength, was calculated from measurements of the reflected intensity of the sample referenced to that of an uncoated silicon wafer. To determine the fringe position, a Lorentzian function was fitted to the measured ITF as shown in Fig. 3(b). The voltage was varied from 0 V to 600 V in steps of 10 V and the resulting fringe shift was measured. At each voltage, 20 reflectivity spectra were averaged. Equation (6) was fitted to the measured data, as shown in Fig. 3(c).

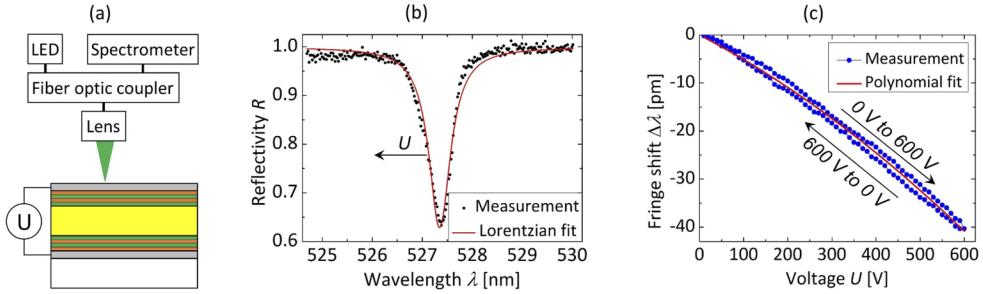

Fig. 3. Measurement scheme for determining the nonlinear optical properties of EO polymers. (a) The light from an LED was focused onto the FP etalon and spectra of the reflected intensity were acquired. (b) Measured ITF of an FP etalon and a Lorentzian function fitted to the data to estimate the center wavelength of the fringe position. (c) To determine the EO properties of the polymer, the fringe shift was recorded as a function of the electrical voltage applied to the electrodes of the FP etalon. A second order polynomial regression model Eq. (6) was fitted to the measurement to determine the Pockels coefficient r_{13} and the Kerr coefficient R_{13}.

The first measurement was made 10 min after poling. The fringe shift as a function of the applied voltage was measured in each sample at five different points and five measurements were carried out at each measurement position, before and after electrical poling.

To determine the poling efficiency, an etalon with the host polymer PVCi and an etalon with the host polymer PMMA each with an MNA content of 10 wt% were measured over an extended voltage range of −1000 V to +1000 V.

4. Results and discussion

Figure 4(a) shows the measured reflectivity R of a DBR consisting of eight alternating layers of SiO_2 and TiO_2, which was calculated from a measurement of its transmission. The absorption of the ITO layer was neglected due to the low extinction coefficient of $k_{ITO}(538\,\text{nm}) = 0.0095$.

The refractive index n and the extinction coefficient k of the PVCi doped with 10 wt% MNA are shown in Figure 4(b). It can be seen that the EO polymer is highly transparent for wavelengths above 450 nm. The EO effects, i.e. the modulation of n, are therefore off-resonant within the studied wavelength range from 500 nm to 575 nm and residual effects due to absorption can be neglected. The inset shows the chemical structure of the guest-host system.

Figure 5 shows the EO coefficients and the change in the refractive index of the PVCi/MNA polymer as a function of the MNA concentration before and after electrical poling. The layer thickness is in the range of $d_{EO} = 5.4 - 5.7\,\mu\text{m}$ and the effective voltage ratio is in the range of $\mu = 0.814 - 0.823$. For the unpoled EO polymers, the Pockels coefficient r_{13} (Fig. 5(a)), the Kerr coefficient R_{13} (Fig. 5(b)), and thus also the resulting change in refractive index Δn (Fig. 5(c)), increase with MNA concentration. After poling, a clear increase in the Pockels coefficient can be seen for all concentrations (blue line Fig. 5(a)) up to a concentration of 10 wt% where

Optical Materials EXPRESS

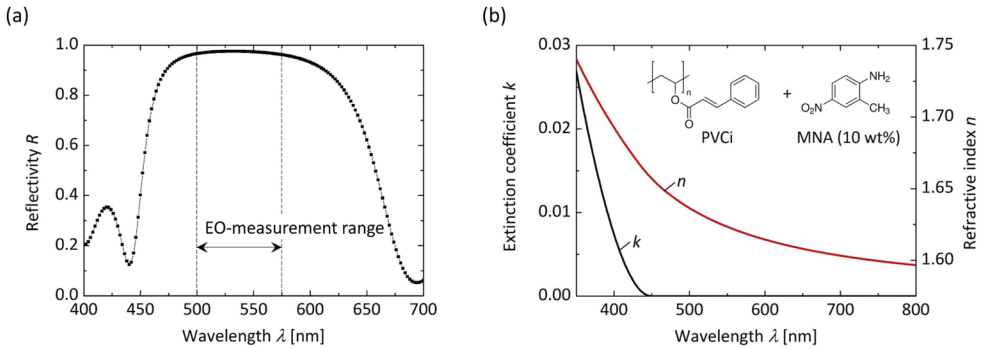

Fig. 4. (a) Reflectivity of the DBR with ITO electrode on a glass substrate. The DBR consists of eight alternating layers of the dielectric materials SiO_2 and TiO_2. The reflectivity in the wavelengths range of the EO measurements is between $R = 0.96$ and $R = 0.98$. (b) Refractive index n and extinction coefficient k of the EO polymer PVCi + 10 wt% MNA. The inset shows the structural formulas of PVCi and MNA.

$r_{13} = (0.547 \pm 0.008)\,\mathrm{pmV^{-1}}$ after which the Pockels coefficient appears to reach a plateau. It is also noticeable that pure PVCi, i.e. $c_{\mathrm{MNA}} = 0\,\mathrm{wt\%}$ in Figure 5(a), exhibits a considerable residual Pockels coefficient of $r_{13} = (0.340 \pm 0.008)\,\mathrm{pmV^{-1}}$, which is increased by a factor of only 1.6 when the chromophore is added. The Pockels coefficient of pure PVCi results from the molecular hyperpolarizability β of the cinnamoyl group [30]. Since the Kerr coefficient does not require acentric molecular order, it is roughly the same before and after electrical poling (Fig. 5(b)). The refractive index change at $U = 600\,\mathrm{V}$ measured in poled FP etalons shows a maximum at 10 wt% MNA and is equivalent to $\Delta n = (-1.483 \pm 0.007) \cdot 10^{-4}$, which agrees with the change in the Pockels coefficient r_{13} (Fig. 5(a)). At higher MNA concentrations, the Pockels effect and the change in the refractive index decreases due to increased dipole-dipole interactions [11]. The contribution of the Pockels coefficient (not shown in Fig. 5(c)) is $\Delta n_{\mathrm{Pockels}} = (-1.081 \pm 0.015) \cdot 10^{-4}$ and that of the Kerr coefficient is $\Delta n_{\mathrm{Kerr}} = (-0.402 \pm 0.013) \cdot 10^{-4}$. Given the relatively high electric field strengths of $E = 91.2\,\mathrm{MV\ m^{-1}}$ across the FP etalon, the Kerr coefficient accounts for 27% of the total change in the refractive index. This result would therefore contradict the common assumption that the Kerr effect can be neglected and may need to be accounted for in EO polymers designed for the visible wavelength region.

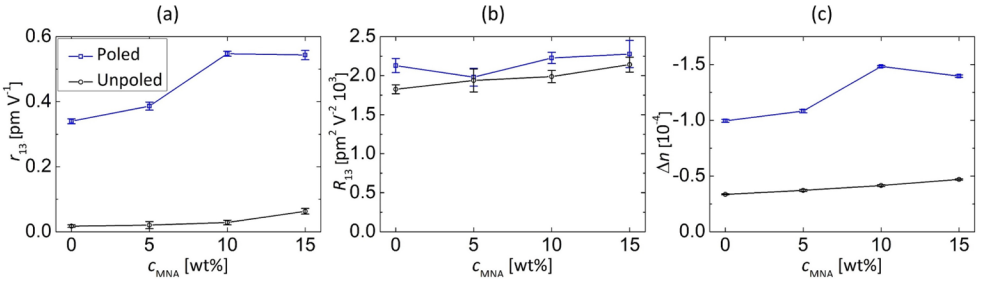

Fig. 5. EO coefficients of the EO polymer consisting of PVCi and MNA as a function of MNA concentration before and after electrical poling. (a) Pockels coefficient r_{13}, (b) Kerr coefficient R_{13} and (c) change in the refractive index Δn for an applied voltage of $U = 600\,\mathrm{V}$.

It should be noted that electro-mechanical effects, which have been neglected here, may also play role, especially for small values of r_{13} [31]. Meyrueix, et al. [22] showed that the Pockels effect is induced by the inverse piezoelectric effect in amorphous polymers containing

Optical Materials EXPRESS

permanent dipoles. However, the setups required to separate EO from electro-mechanical effects are considerably more complex [21,32,33] and were therefore outside the remit of this study.

Table 1 shows the Pockels and Kerr coefficients for guest-host systems with PVCi and with PMMA as the host polymer. The EO polymer with PMMA shows a significantly larger Pockels coefficient before and after poling than that with PVCi. PMMA + 10 wt% MNA has a Pockels coefficient of $r_{13} = (1.735 \pm 0.029)\,\mathrm{pmV^{-1}}$ after poling. This is an increase by a factor of 3.17 compared to PVCi + 10 wt% MNA. The host polymer therefore has a significant influence on the Pockels effect in guest-host systems. Similar to PVCi, pure PMMA shows an inherent Pockels effect with $r_{13} = (0.085 \pm 0.018)\,\mathrm{pmV^{-1}}$ for the unpoled material. This is five times greater than that of unpoled pure PVCi, while the poled pure polymers produced similar Pockels effects around $r_{13} = 0.34 - 0.40\,\mathrm{pmV^{-1}}$. These values deviate from those reported by Bouclé et al. who reported an effective Pockels coefficient of $r_e = (0.10 \pm 0.01)\,\mathrm{pmV^{-1}}$ and $r_e = (0.20 \pm 0.01)\,\mathrm{pmV^{-1}}$ for unpoled and poled PMMA, respectively [34]. Assuming that the effective Pockels coefficient r_e corresponds roughly to r_{13} reported here, the deviations may be explained by different poling conditions and the omission of the Kerr effect. The latter increases slightly for pure PMMA as a result of electrical poling and is comparable to the values of PVCi. By contrast, the Kerr coefficient of the unpoled guest-host system PMMA + 10 wt% MNA with $R_{13} = (4819 \pm 90)\,\mathrm{pm^2V^{-2}}$ is significantly higher than that of PVCi + 10 wt% MNA. The Pockels coefficients reported in this work could be increased further by optimizing the poling procedure.

Table 1. Pockel coefficient r_{13} and Kerr coefficient R_{13} for the guest-host systems PVCi + MNA and PMMA + MNA with different concentrations of EO chromophore for poled and unpoled FP etalons.

	$r_{13}[\mathrm{pmV^{-1}}]$		$R_{13}[\mathrm{pm^2V^{-2}}]$	
	unpoled	poled	unpoled	poled
PVCi	0.017±0.004	0.340±0.008	1826±56	2129±90
PVCi + 5 wt% MNA	0.021±0.011	0.387±0.013	1939±147	1981±114
PVCi + 10 wt% MNA	0.029±0.007	0.547±0.008	1989±78	2227±72
PVCi + 15 wt% MNA	0.063±0.009	0.543±0.014	2142±95	2277±172
PMMA	0.085±0.018	0.397±0.017	1718±168	2076±150
PMMA + 10 wt% MNA	0.404±0.017	1.735±0.029	4819±90	3359±198

The longterm orientational stability of the EO chromophores, which can affect functionality, can be improved by thermal or photochemical crosslinking of the host polymer during the poling process. This would process to lead to a higher temporal stability of the Pockels effect. In a separate study, we have found that the degree of photochemical crosslinking of PVCi has no influence on the EO properties of the guest-host system used in this work [13]. Crosslinking was not used in this work. These results do not agree with those reported by Mandal et al. [4], who demonstrated that the crosslinking of PVCi improve the orientational stability and thus on the EO properties. The discrepancy may be explained by the much larger EO chromophore (3-cinnamoyloxy-4-[4-(N,N-diethylamino)-2-cinnamoyloxy phenylazo] nitrobenzene) used in their work.

Figure 6 shows the fringe shift as a function of the applied voltage for the poled and unpoled EO polymers consisting of either PVCi (Fig. 6(a)) or PMMA (Fig. 6(b)) with 10 wt% MNA. The poling shifts the apex of the parabola in the direction of the poling voltage and induces a positive fringe shift in the FP etalon. A significantly larger shift of the apex of the sample based on PMMA compared to PVCi was observed. For the poled PMMA sample, the apex is located at $U = -375$ V while the poled PVCi sample produced a peak at $U = -239$ V. The increased shift of the apex suggests a more effective poling process, which in turn leads to a stronger Pockels effect. The increased Kerr effect, evident from the steeper slope of the parabola, also amplifies the Pockels effect in poled polymers. A slight hysteresis can be seen with the EO polymer

Optical Materials EXPRESS

PMMA + 10 wt% MNA, and especially with positive measurement voltages. The precise cause for the hysteresis could not be established but it is possible that space charges, which are located at the interfaces between the DBR and the EO polymer may explain these observations.

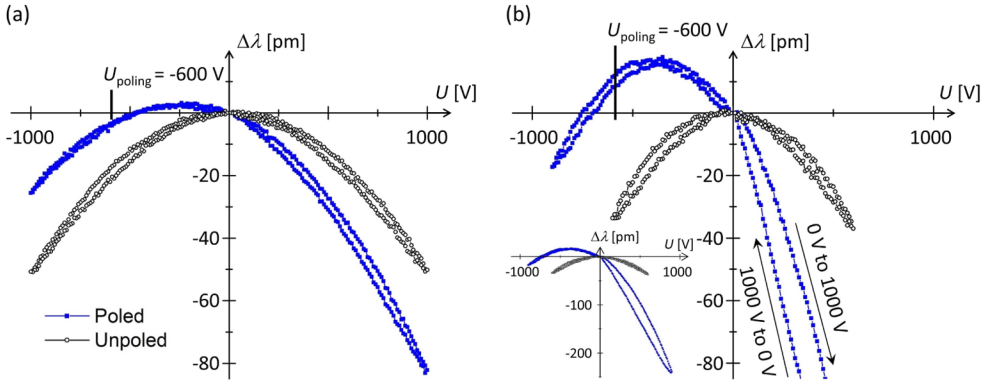

Fig. 6. Fringe shift $\Delta\lambda$ as a function of the applied voltage U for the poled (blue) and unpoled (black) EO polymers (a) PVCi + 10 wt% MNA and (b) PMMA + 10 wt% MNA. The inset shows the fringe shift for the entire voltage range.

Figure 7 shows the EO coefficients and the change in the refractive index measured using an FP etalon as a function of the number of DBR layers between the electrode and the EO polymer (PVCi with 10 wt% MNA). The effective voltage ratio was calculated using equation 3 as $\mu = 1$ for $N = 0$, $\mu = 0.891$ for $N = 4$ and $\mu = 0.814$ for $N = 8$. The layer thickness of the EO polymer was in the range of $d_{EO} = 5.4 - 5.5\,\mu m$. The measurements were made on unpoled FP etalons up to a maximum voltage of $U = 400\,V$. Since the voltage drop at the DBR is taken into account when calculating the Pockels and the Kerr coefficient, the coefficients are independent of the number of layers of the DBR, which is apparent from Figure 7(a) and 7(b). The change in the refractive index decreases continuously with an increasing number of layers, which can be seen in Fig. 7(c), since the electric field strength within the EO polymer decreases.

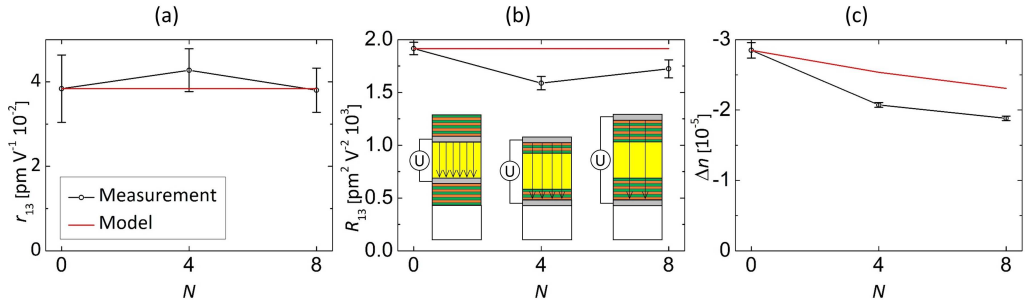

Fig. 7. EO coefficients as a function of the number of DBR layers between the electrode and the EO polymer PVCi + 10 wt% MNA for unpoled FP etalons. (a) Pockels coefficient r_{13}, (b) Kerr coefficient R_{13} and (c) change in the refractive index Δn for an applied voltage of $U = 400\,V$. The inset in (b) shows schematically the structure of the FP etalons used for the measurements.

5. Conclusion

This paper reports the EO properties of PVCi and PMMA polymers doped with varying concentrations of MNA. The resulting guest-host systems are transparent at wavelengths greater

Optical Materials EXPRESS

than 450 nm. The Pockels coefficient of the poled EO polymer with PVCi as host polymer was found to increase with MNA concentration, showing a maximum of $r_{13} = (0.547 \pm 0.008)\,\mathrm{pmV^{-1}}$ at 10 wt%. By contrast, the PMMA-based EO polymer exhibited a maximum Pockels coefficient of $r_{13} = (1.735 \pm 0.029)\,\mathrm{pmV^{-1}}$. It was found that the host material has a strong impact on the poling efficiency and the EO properties of guest-host systems. In addition, undoped host polymers showed a significant Pockels coefficient of similar value ($r_{13} = (0.340 \pm 0.008)\,\mathrm{pmV^{-1}}$ for PVCi, $r_{13} = (0.397 \pm 0.017)\,\mathrm{pmV^{-1}}$ for PMMA). It was found that the Kerr coefficient contributes significantly to the total EO change in refractive index in poled EO polymers, especially at high electric field strengths. Transparent visible EO polymers may find application in tuneable FP sensors for optical ultrasound detection, tuneable optical filters, high-resolution spectrometers and spatial light modulators in the visible spectral range.

Funding. Deutsche Forschungsgemeinschaft (283368314); Open Access Publication Funds of the Technische Hochschule Wildau – Technical University of Applied Sciences.

Disclosures. The authors declare that there are no conflicts of interest related to this article.

Data availability. Data underlying the results presented in this paper are not publicly available at this time but may be obtained from the authors upon reasonable request.

References

1. G. A. Lindsay, M. C. Davis, A. P. Chafin, S. Fallis, R. C. Hoffman, T. M. Pritchett, J. Andzelm, A. M. Rawlett, D. Park, and W. N. Herman, "Electro-optic polymeric films of phenylethynyl dyes with transparency in the blue region of the visible spectrum," Opt. Mater. **32**(2), 302–310 (2009).
2. M. Eich, A. Sen, H. Looser, G. C. Bjorklund, J. D. Swalen, R. Twieg, and D. Y. Yoon, "Corona poling and real–time second–harmonic generation study of a novel covalently functionalized amorphous nonlinear optical polymer," J. Appl. Phys. **66**(6), 2559–2567 (1989).
3. H. Xu, F. Liu, D. L. Elder, L. E. Johnson, Y. de Coene, K. Clays, B. H. Robinson, and L. R. Dalton, "Ultrahigh electro-optic coefficients, high index of refraction, and long-term stability from diels–alder cross-linkable binary molecular glasses," Chem. Mater. **32**(4), 1408–1421 (2020).
4. B. K. Mandal, Y. M. Chen, J. Y. Lee, J. Kumar, and S. Tripathy, "Cross–linked stable second–order nonlinear optical polymer by photochemical reaction," Appl. Phys. Lett. **58**(22), 2459–2460 (1991).
5. W. Heni, Y. Kutuvantavida, C. Haffner, H. Zwickel, C. Kieninger, S. Wolf, M. Lauermann, Y. Fedoryshyn, A. F. Tillack, L. E. Johnson, D. L. Elder, B. H. Robinson, W. Freude, C. Koos, J. Leuthold, and L. R. Dalton, "Silicon–organic and plasmonic–organic hybrid photonics," ACS Photonics **4**(7), 1576–1590 (2017).
6. C.-C. Chang, C.-P. Chen, C.-C. Chou, W.-J. Kuo, and R.-J. Jeng, "Polymers for electro–optical modulation," J. Macromol. Sci., Polym. Rev. **45**(2), 125–170 (2005).
7. X. Cheng, F. Qiu, A. M. Spring, M. Sasaki, T. Kashino, M. Ozawa, H. Nawata, T. Kita, O. Sugihara, and S. Yokoyama, "Camera sensor platform for high speed video data transmission using a wideband electro-optic polymer modulator," Opt. Express **27**(3), 1877–1883 (2019).
8. C. Greenlee, J. Luo, K. Leedy, B. Bayraktaroglu, R. A. Norwood, M. Fallahi, A. K.-Y. Jen, and N. Peyghambarian, "Electro-optic polymer spatial light modulator based on a fabry-perot interferometer configuration," Opt. Express **19**(13), 12750–12758 (2011).
9. J. Liu, C. Ouyang, F. Huo, W. He, and A. Cao, "Progress in the enhancement of electro-optic coefficients and orientation stability for organic second-order nonlinear optical materials," Dyes Pigm. **181**, 108509 (2020).
10. L. Dalton and S. Benight, "Theory-guided design of organic electro-optic materials and devices," Polymers **3**(3), 1325–1351 (2011).
11. L. R. Dalton, P. A. Sullivan, and D. H. Bale, "Electric field poled organic electro-optic materials: state of the art and future prospects," Chem. Rev. **110**(1), 25–55 (2010).
12. T. Verbiest, S. Houbrechts, M. Kauranen, K. Clays, and A. Persoons, "Second-order nonlinear optical materials: recent advances in chromophore design," J. Mater. Chem. **7**(11), 2175–2189 (1997).
13. C. Villringer, T. Saeb Gilani, E. Z. Zhang, S. Pulwer, P. Steglich, S. Schrader, and J. Laufer, "Development of tuneable fabry-pérot sensors for parallelised photoacoustic signal acquisition," in *Photons Plus Ultrasound: Imaging and Sensing 2019*, A. A. Oraevsky and L. V. Wang, eds. (SPIE, 02.02.2019 - 07.02.2019), p. 21.
14. T. Saeb Gilani, J. Laufer, C. Villringer, E. Z. Zhang, H. Gundlach, J. Buchmann, and S. Schrader, "Parallelised photoacoustic signal acquisition using a fabry-perot sensor and a camera-based interrogation scheme," in *Photons Plus Ultrasound: Imaging and Sensing 2018*, A. A. Oraevsky and L. V. Wang, eds. (SPIE, 27.01.2018 - 01.02.2018), p. 104.
15. J. Buchmann, J. Guggenheim, E. Zhang, C. Scharfenorth, B. Spannekrebs, C. Villringer, and J. Laufer, "Characterization and modeling of fabry-perot ultrasound sensors with hard dielectric mirrors for photoacoustic imaging," Appl. Opt. **56**(17), 5039–5046 (2017).

Optical Materials EXPRESS

16. E. Zhang, J. Laufer, and P. Beard, "Backward-mode multiwavelength photoacoustic scanner using a planar fabry-perot polymer film ultrasound sensor for high-resolution three-dimensional imaging of biological tissues," Appl. Opt. **47**(4), 561–577 (2008).
17. J. Zyss, "Organic crystals and quadratic nonlinear optics: The transparency-efficiency trade-off," in *Conjugated Polymeric Materials: Opportunities in Electronics, Optoelectronics, and Molecular Electronics*, J. L. Brédas and R. R. Chance, eds. (Springer Netherlands, 1990), NATO ASI Series, pp. 545–557.
18. H. S. Nalwa and S. Miyata, *Nonlinear Optics of Organic Molecules and Polymers* (CRC, 1997).
19. M. G. Kuzyk, 1958, C. W. Dirk, and 1954, *Characterization Techniques and Tabulations for Organic Nonlinear Optical Materials* (Marcel Dekker, 1998).
20. R. Sudharsanam, S. Chandrasekaran, and P. K. Das, "Unsymmetrical aryl disulfides with excellent transparency in the visible region for second order nonlinear optics," J. Mater. Chem. **12**(10), 2904–2908 (2002).
21. C. A. Eldering, A. Knoesen, and S. T. Kowel, "Use of fabry–pérot devices for the characterization of polymeric electro–optic films," J. Appl. Phys. **69**(6), 3676–3686 (1991).
22. R. Meyrueix and O. Lemonnier, "Piezoelectrically induced electro-optical effect and dipole orientation measurement in undoped amorphous polymers," J. Phys. D: Appl. Phys. **27**(2), 379–386 (1994).
23. H. Gan, H. Zhang, C. T. DeRose, R. A. Norwood, N. Peyghambarian, M. Fallahi, J. Luo, B. Chen, and A. K.-Y. Jen, "Low drive voltage fabry-pérot étalon device tunable filters using poled hybrid sol-gel materials," Appl. Phys. Lett. **89**(4), 041127 (2006).
24. H. G. Tompkins, ed., *Handbook of Ellipsometry* (Andrew, 2010), repr ed.
25. S. Murase, K. Kinoshita, K. Horie, and S. Morino, "Photo-optical control with large refractive index changes by photodimerization of poly(vinyl cinnamate) film," Macromolecules **30**(25), 8088–8090 (1997).
26. I. Assaid, D. Bosc, and I. Hardy, "Improvements of the poly(vinyl cinnamate) photoresponse in order to induce high refractive index variations," J. Phys. Chem. B **108**(9), 2801–2806 (2004).
27. D. A. G. Bruggeman, "Berechnung verschiedener physikalischer konstanten von heterogenen substanzen. i. dielektrizitätskonstanten und leitfähigkeiten der mischkörper aus isotropen substanzen," Ann. Phys. **416**(7), 636–664 (1935).
28. H. Fujiwara, *Spectroscopic Ellipsometry: Principles and Applications* (John Wiley & Sons, Ltd, 2007).
29. G. E. Jellison and F. A. Modine, "Parameterization of the optical functions of amorphous materials in the interband region," Appl. Phys. Lett. **69**(3), 371–373 (1996).
30. I. Drevenšek Olenik, M. W. Kim, A. Rastegar, and T. Rasing, "Probing photo-induced alignment in poly(vinyl cinnamate) films by surface second-harmonic generation," Appl. Phys. B: Lasers Opt. **68**(3), 599–603 (1999).
31. R. A. Norwood, M. G. Kuzyk, and R. A. Keosian, "Electro–optic tensor ratio determination of side–chain copolymers with electro–optic interferometry," J. Appl. Phys. **75**(4), 1869–1874 (1994).
32. C. Greenlee, A. Guilmo, A. Opadeyi, R. Himmelhuber, R. A. Norwood, M. Fallahi, J. Luo, S. Huang, X.-H. Zhou, A. K.-Y. Jen, and N. Peyghambarian, "Mach–zehnder interferometry method for decoupling electro-optic and piezoelectric effects in poled polymer films," Appl. Phys. Lett. **97**(4), 041109 (2010).
33. H.-J. Winkelhahn and D. Neher, "Electro-optical and electro-mechanical properties of poled polymer films," in *Nonlinear Optical Properties of Organic Materials VII*, G. R. Moehlmann, ed. (SPIE, 1994), SPIE Proceedings, pp. 41–48.
34. J. Bouclé, A. Kassiba, M. Makowska-Janusik, N. Herlin-Boime, C. Reynaud, A. Desert, J. Emery, A. Bulou, J. Sanetra, A. A. Pud, and S. Kodjikian, "Linear electro-optical behavior of hybrid nanocomposites based on silicon carbide nanocrystals and polymer matrices," Phys. Rev. B **74**(20), 205417 (2006).